Synthesis, characterisation, reactivity and *in vitro* antiamoebic activity of hydrazone based oxovanadium(IV), oxovanadium(V) and μ-bis(oxo)bis{oxovanadium(V)} complexes

Mannar R. Maurya,*[a] Shalu Agarwal,[a] Mohammad Abid,[b] Amir Azam,[b] Cerstin Bader,[c] Martin Ebel[c] and Dieter Rehder[c]

Received 31st August 2005, Accepted 13th October 2005
First published as an Advance Article on the web 7th November 2005
DOI: 10.1039/b512326g

Binuclear, μ-bis(oxo)bis{oxovanadium(V)} complexes $[(VOL)_2(\mu\text{-}O)_2]$ (**2** and **7**) (where HL are the hydrazones Hacpy-nah **I** or Hacpy-fah **II**; acpy = 2-acetylpyridine, nah = nicotinic acid hydrazide and fah = 2-furoic acid hydrazide) were prepared by the reaction of $[VO(acac)_2]$ and the ligands in methanol followed by aerial oxidation. The paramagnetic intermediate complexes [VO(acac)(acpy-nah)] (**1**) and [VO(acac)(acpy-fah)] (**6**) have also been isolated. Treatment of [VO(acac)(acpy-nah)] and [VO(acac)(acpy-fah)] with aqueous H_2O_2 yields the oxoperoxovanadium(V) complexes $[VO(O_2)(acpy\text{-}nah)]$ (**3**) and $[VO(O_2)(acpy\text{-}fah)]$ (**8**). In the presence of catechol (H_2cat) or benzohydroxamic acid (H_2bha), **1** and **6** give the mixed chelate complexes [VO(cat)L] (HL = **I**: **4**, HL = **II**: **9**) or [VO(bha)L] (HL = **I**: **5**, HL = **II**: **10**). Complexes **4**, **5**, **9** and **10** slowly convert to the corresponding oxo-μ-oxo species **2** and **7** in DMF solution. Ascorbic acid enhances this conversion under aerobic conditions, possibly through reduction of these complexes with concomitant removal of coordinated catecholate or benzohydroxamate. Acidification of **7** with HCl dissolved in methanol afforded a hydroxo(oxo) complex. The crystal and molecular structure of $\mathbf{2}\cdot 1.5H_2O$ has been determined, and the structure of **7** re-determined, by single crystal X-ray diffraction. Both of these binuclear complexes contain the uncommon asymmetrical $\{VO(\mu\text{-}O)\}_2$ diamond core. The *in vitro* tests of the antiamoebic activity of ligands **I** and **II** and their binuclear complexes **2** and **7** against the protozoan parasite *Entamoeba histolytica* show that the ligands have no amoebicidal activity while their vanadium complexes **2** and **7** display more effective amoebicidal activity than the most commonly used drug metronidazole (IC_{50} values are 1.68 and 0.45 μM, respectively *vs* 1.81 μM for metronidazole). Complexes **2** and **7** catalyse the oxidation of styrene and ethyl benzene effectively. Oxidation of styrene, using H_2O_2 as an oxidant, gives styrene epoxide, 2-phenylacetaldehyde, benzaldehyde, benzoic acid and 1-phenyl-ethane-1,2-diol, while ethyl benzene yields benzyl alcohol, benzaldehyde and 1-phenyl-ethane-1,2-diol.

Introduction

Hydrazone moieties are the most important pharmacophoric cores of several antiinflammatory, antinociceptive, and antiplatelet drugs.[1] The biological profile of compounds presenting this subunit is related to its relative acidity and its capacity to stabilise free radicals, thus mimicking the bisallyl fragment of certain unsaturated fatty acids, which contribute to the inhibition of the active site of oxidatively catabolic enzymes such as cyclooxygenase and 5-lypooxygenase, which in turn are responsible for the biosynthesis of prostaglandins, thromboxanes, and leucotrienes.[2] On the other hand, the coordination chemistry of vanadium[3] has received considerable attention since the discovery of vanadium in the vanadium-dependent haloperoxidases,[4] nitrogenases[5] and nitrate reductases.[6] Its biological significance is further exemplified by its incorporation in natural products (amavadin in *Amanitae* mushrooms[7]), blood cells of sea-squirts (*Ascidiaceae*) and fan worms,[8] and by its potency as an inhibitor of phosphoryl transfer enzymes.[9] Several vanadium compounds have been shown to be active as insulin mimetics *in vitro* and *in vivo*,[10] including clinical tests, demonstrating the usability of simple inorganic (vanadyl sulfate, vanadate) and coordination compounds ($[VO(maltolato)_2]$) for the treatment of diabetes mellitus in humans.[11,12]

Protozoa that parasitise the human intestines causing disease include *Entamoeba histolytica*, *Giardia lamblia* and other spore-forming protozoa. The intestinal parasite *Entamoeba*, the causative agent of amoebiasis, is responsible for amoebic colitis and amoebic liver abscesses. This disease afflicts millions of individuals in developing countries. The WHO in its most recent estimates has placed the death toll from amoebiasis at 40 000–100 000 lives annually.[13] Nitroimidazoles, particularly metronidazole, is the mainstay of therapy for invasive amoebiasis. Approximately 90% of patients having mild to moderate amoebic dysentery respond to nitroimidazole treatment. Side effects are, however,

[a]*Department of Chemistry, Indian Institute of Technology Roorkee, Roorkee, 247 667, India. E-mail: rkmanfcy@iitr.ernet.in*
[b]*Department of Chemistry, Jamia Milia Islamia, Jamia Nagar, New Delhi, 100025, India*
[c]*Institut für Anorganische und Angewandte Chemie, Universität Hamburg, Martin-Luther-King-Platz 6, 20146, Hamburg, Germany*

common and include a disulfiram-like reaction (predominantly nausea and vomiting) when taken with alcohol, in addition to a dry mouth and headache.[14] *Entamoeba* strains resistant to this drug have also begun to appear.[15] It is therefore desirable to search for new and effective amoebicidals. Combining the pharmocophoric efficacy of the hydrazone core and the potential medicinal effect of vanadium compounds, we have recently begun a programme directed towards the study of the antiamoebic activity of hydrazone based and related vanadium coordination compounds, and obtained promising results for their *in vitro* activity.[16]

In this paper, we describe the synthesis and characterisation of oxovanadium(IV) oxovanadium(V) and μ-bis(oxo)bis{oxovanadium(V)} complexes of the hydrazones **I** and **II** derived from acetylpyridine (acpy) and nicotinic acid hydrazide (Hnah) or 2-furoic acid hydrazide (Hfah); Scheme 1. The antiamoebic screening of μ-bis(oxo)bis{oxovanadium(V)} complexes against HM1:1MSS strains of *Entamoeba histolytica* is reported here. As many vanadium complexes show catalytic activity in oxidation and oxygen transfer reactions,[17,18] including the oxidation of (prochiral) organic sulfides to (chiral) sulfoxides,[19–22] thus modelling the haloperoxidase activity, related reactivity patterns have also been studied by testing the catalytic activity of some of the complexes with respect to the oxidation of styrene and ethyl benzene, using H_2O_2 as an oxidant. Oxidation reactions of various organic substrates by peroxides, catalysed by vanadium complexes, have been reviewed.[23]

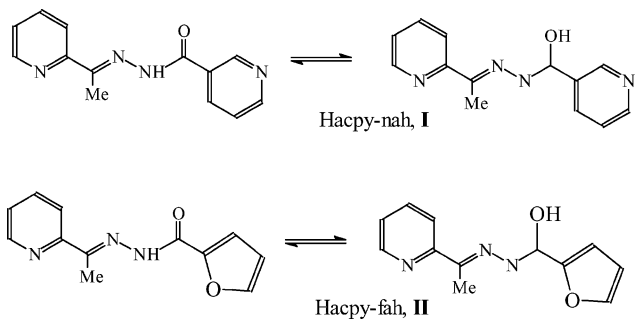

Scheme 1

Experimental

Materials and methods

V_2O_5, catechol (H_2cat), benzohydroxamic acid (H_2bha) (Loba Chemie, India), nicotinic acid hydrazide, 2-furoic acid hydrazide (Fluka Chemie GmbH, Switzerland), acetylacetone (Hacac), 2-acetylpyridine (Aldrich, USA) and 30% aqueous H_2O_2 (Qualigens, India) were used as obtained. Other chemicals and solvents were of analytical reagent grade. [VO(acac)$_2$] was prepared as described in the literature.[24]

Thermogravimetric analyses of the complexes were carried out under oxygen atmosphere using a TG Stanton Redcroft STA 780 instrument. The magnetic susceptibilities of oxovanadium(IV) complexes were measured at 298 K with a Vibrating Sample Magnetometer model 155, using nickel as standard. Diamagnetic corrections were carried out using Pascal's increments.[25] Elemental analyses of the ligands and complexes were performed by an Elementar model Vario-EI-III. IR spectra were recorded as KBr pellets on a Perkin–Elmer 1600 FT-IR spectrometer. Electronic absorption spectra were measured in methanol or DMF with an UV-1601 PC UV/Vis spectrophotometer. ^{1}H NMR spectra were obtained on Bruker 200, and ^{51}V NMR spectra on a Bruker Avance 400 MHz spectrometer at 94.73 MHz with the common parameter settings. NMR spectra were usually recorded in DMSO-d_6, and $\delta(^{51}V)$ values are referenced relative to $VOCl_3$ as external standard. EPR spectra were recorded with a Bruker ESP 300E spectrometer between 9.42 and 9.47 GHz, and EPR parameters were adjusted by simulation with the Bruker program system SimFonia. Cyclic voltammetric experiments were carried out in acetonitrile using a platinum working and Ag–AgCl reference electrode on a Basic Electrochemistry System model ECDA 001 of Con Serve Enterprises, India. Products of the catalytically conducted reactions analysed quantitatively by a gas chromatograph (Hewlett Packard 5890, FID Detector, HP-1 packed column), and the identities of the products confirmed by GC-MS (Perkin-Elmer, Clasus 500).

Crystal structure data were collected on a Bruker SMART Apex CCD diffractometer at 153(2) K, using a graphite monochromator and Mo Kα radiation (λ = 0.71073 Å). Hydrogen atoms were placed into calculated positions and included in the last cycles of refinement. The program systems SHELXS 86 and SHELXL 93 were used throughout. Crystal and refinement data for complex **2** (the compound contained 1.5 highly disordered solvent molecules, possibly water, represented by O100, O200 and O300 in the atomic coordinates map, which have not been considered in the following data collection): Empirical formula $C_{26}H_{25}N_8O_{7.5}V_2$, formula weight, 671.42 g mol^{-1}, monoclinic crystal system *C2/c*. Unit cell dimensions: a = 23.9504(7) Å, b = 15.1397(4) Å, c = 7.7450(2) Å, β = 102.4840(10)°. Cell volume = 2741.95(13) Å^3, Z = 4, ρ_{calc} = 1.626 g cm^{-3}; μ = 0.746 mm^{-1}. Crystal size: 0.72 × 0.36 × 0.24 mm^3. F(000) 1372, θ range for data collection 2.69 to 32.54°, index ranges $-36 \leq h \leq 30$, $-22 \leq k \leq 18$, $-11 \leq l \leq 11$, reflections collected 19 955, independent reflections 4906 (R_{int} = 0.0343), completeness to θ = 32.54°: 98.3%, data/restraints/parameters 4906/3/211. Goodness-of-fit on F^2 1.054, final R indices [$I>2\sigma(I_0)$]: $R1$ = 0.0408, $wR2$ = 0.1130, R indices (all data): $R1$ = 0.0486, $wR2$ = 0.1165; largest diff. peak and hole 0.639 and −0.345 e Å^{-3}. Our data on the structure of compound **7** conform to those published previously.[26]

CCDC reference numbers: **2**: 282762, **7**: 267177.

For crystallographic data in CIF or other electronic format see DOI: 10.1039/b512326g.

Preparation of ligands

Hacpy-nah I. A hot solution of nicotinic acid hydrazide (1.37 g, 10 mmol) in 50 mL of methanol was treated with 2-acetylpyridine(1.22 g, 10 mmol) in 50 mL of methanol, and the reaction mixture was gently heated under reflux on a water bath for 4 h. After reducing the solvent to *ca.* 15 mL and cooling to rt for 2 h, the precipitated white solid was filtered off, washed with methanol and dried. Finally, it was recrystallised from methanol. Yield 1.93 g (80%). (Found: C, 64.68; H, 5.11; N, 23.13. Calc. for $C_{13}H_{12}N_4O$: C, 64.99; H, 5.03; N, 23.32%). IR (KBr, ν_{max}): 3191(NH), 1669 (C=O), 1619, 1588 (C=N$_{azomethine}$, C=N$_{ring}$), 990 cm^{-1} (N–N).

Hacpy-fah II. This was prepared by following the same procedure outlined for Hacpy-nah. The pure product was obtained

as a white solid. Yield after crystallisation from methanol 1.69 g (74%). (Found: C, 63.10; H, 4.93; N, 18.22. Calc. for $C_{12}H_{11}N_3O_2$: C, 62.87; H, 4.84; N, 18.33%). IR (KBr, ν_{max}): 3181(NH), 1678 (C=O), 1591, 1580 (C=$N_{azomethine}$, C=N_{ring}), 1009 cm^{-1} (N–N).

Preparation of complexes

[VO(acac)(acpy-nah)] 1. A stirred solution of Hacpy-nah (0.48 g, 2 mmol) in dry methanol (20 mL) was treated with [VO(acac)$_2$] (0.53 g, 2 mmol) dissolved in the same solvent (20 mL) and the resulting mixture was heated under reflux for 4 h. The green solid that separated on cooling the reaction flask to ambient temperature was filtered off, washed with methanol and dried *in vacuo*. Yield 0.62 g (77%). (Found: C, 52.98; H, 4.37; N, 13.76. Calc. for $C_{18}H_{18}N_4O_4V$: C, 53.34; H, 4.48; N, 13.82%). IR (KBr, ν_{max}): 1589, 1580 (C=$N_{azomethine}$, C=N_{ring}), 1277 (C–$O_{enolate}$), 1029 (N–N), 958 cm^{-1} (V=O). μ_{eff} (293 K) = 1.70 μ_B.

[{VO(acpy-nah)}$_2$(μ-O)$_2$] 2.

Method A. Complex **1**(0.80 g, 2 mmol) was suspended in 80 mL of methanol and air was passed through the solution with occasional shaking and heating at *ca.* 50 °C until the green residual material slowly dissolved and crystalline yellow solid **2** separated instead. This was filtered off, washed with methanol and dried *in vacuo*. Yield 0.46 g (71%). (Found: C, 48.96; H, 3.42; N, 17.60. Calc. for $C_{26}H_{22}N_8O_6V_2$: C, 48.46; H, 3.44; N, 17.39%). IR (KBr, ν_{max}): 1600, 1582 (C=$N_{azomethine}$, C=N_{ring}), 1266 (C–$O_{enolate}$), 1032 (N–N), 958 (V=O), 778 cm^{-1} [V-(μ-O)-V].

Method B. Vanadium(v) oxide (0.50 g, eqv. 5 mmol vanadium) was dissolved in aqueous KOH (0.336 g, 6 mmol in 10 mL) and stirred for 2 h. The resulting solution was filtered. A filtered solution of Hacpy-nah (1.20 g, 5 mmol), dissolved in 20 mL of aqueous KOH (0.280 g, 5 mmol) was added to the above solution under continuous stirring, slowly adjusting the pH of the reaction mixture to 7.5 with 4 M HCl. After 2 h, the precipitated yellow **2** was filtered off, washed with water and dried. Recrystallisation from methanol gave 0.89 g (55%) of **2**. Analytical and spectral data matched with those given above.

[VO(O$_2$)(acpy-nah)] 3. A methanolic solution of **1** (0.40 g, 1 mmol in 40 mL) was treated with aqueous 30% H_2O_2 (6 mL, 53 mmol) with stirring at ambient temperature, causing darkening of the reaction mixture. After 2 h of stirring, the volume was reduced to *ca.* 10 mL and left overnight at *ca.* 10 °C. Orange-red crystals of **3** were filtered off, washed with cold methanol and dried *in vacuo*. Yield 0.15 g (43%). IR (KBr, ν_{max}): 1601, 1585 (C=$N_{azomethine}$, C=N_{ring}), 1237 (C–$O_{enolate}$), 1025 (N–N), 963 (V=O), 925 (O–O), 773 [$V(O)_{2\ asym}$], 594 cm^{-1} [$V(O)_{2\ sym}$].

[VO(cat)(acpy-nah)] 4. Complex **1** (0.4 g, 1 mmol) was dissolved in hot methanol (40 mL). After cooling the solution to rt, catechol (0.11 g, 1 mmol) was added in one portion and the reaction mixture was stirred for 6 h. The volume of the solvent was reduced to *ca.* 10 mL and the mixture was kept in the refrigerator overnight, whereupon brown-black solid **4** separated out. This was filtered off, washed with cold methanol and dried *in vacuo*. Yield 0.21 g (51%). (Found: C, 54.77; H, 3.45; N, 13.81. Calc. for $C_{19}H_{15}N_4O_4V$: C, 55.08; H, 3.65; N, 13.52%). IR (KBr, ν_{max}): 1597, 1578 (C=$N_{azomethine}$, C=N_{ring}), 1259 (C–$O_{enolate}$), 1023 (N–N), 961 cm^{-1} (V=O).

[VO(bha)(acpy-nah)] 5. Complex **1** (0.4 g, 1 mmol) was dissolved in hot methanol (40 mL) and to this, after cooling to ambient temperature, was added benzohydroxamic acid (0.137 g, 1 mmol). The obtained reaction mixture was stirred for 6 h and then kept overnight at 10 °C after reducing the volume to *ca.* 10 mL. Compound **5** separated out, was filtered off, washed with methanol and dried *in vacuo*. Yield 0.23 g (53%). (Found: C, 53.91; H, 3.63; N, 15.87. Calc for $C_{20}H_{17}N_5O_4V$: C, 54.31; H, 3.87; N, 15.83%). IR (KBr, ν_{max}): 1596, 1581 (C=$N_{azomethine}$, C=N_{ring}), 1258 (C–$O_{enolate}$), 1025 (N–N), 964 cm^{-1} (V=O).

[VO(acac)(acpy-fah)] 6 and [{VO(acpy-fah)}$_2$(μ-O)$_2$] 7. Complexes **6** and **7** were prepared analogously to **1** and **2**, replacing Hacpy-nah for Hacpy-fah. Complex **7** can also be prepared by method B described for **2**.

Data for **6**: Yield 0.56 g (72%). (Found: C, 51.45; H, 4.52; N, 10.45. Calc. for $C_{17}H_{17}N_3O_5V$: C, 51.79; H, 4.35; N, 10.66%). IR (KBr, ν_{max}): 1598, 1581 (C=$N_{azomethine}$, C=N_{ring}), 1227 (C–$O_{enolate}$), 1027 (N–N), 953 cm^{-1} (V=O). μ_{eff} (293 K) = 1.78 μ_B. Data for **7**: Yield 0.44 g (71%). (Found: C, 46.25; H, 3.29; N, 13.47. Calc. for $C_{24}H_{20}N_6O_8V2$: C, 46.32; H, 3.24; N, 13.50%). IR (KBr, ν_{max}): 1598, 1582 (C=$N_{azomethine}$, C=N_{ring}), 1230 (C–$O_{enolate}$), 1043 (N–N), 951 (V=O), 773 cm^{-1} [V–(μ-O)–V].

[VO(O$_2$)(acpy-fah)] 8. Complex **8** was prepared by the procedure described for **3**. Yield 0.15 g (45%). IR (KBr, ν_{max}): 1602, 1584 (C=$N_{azomethine}$, C=N_{ring}), 1228 (C–$O_{enolate}$), 1024 (N–N), 965 (V=O), 926 (O–O), 775 [$V(O)_{2\ asym}$], 593 cm^{-1} [$V(O)_{2\ sym}$].

[VO(cat)(acpy-fah)] 9 and [VO(bha)(acpy-fah)] 10. Complexes **9** and **10** were isolated by reacting **6** with catechol or benzohydroxamic acid, respectively, in methanol as outlined for **4** and **5**. Data for **9**: Yield 0.19 g (48%). (Found: C, 53.35; H, 3.41; N, 10.24. Calc. for $C_{18}H_{14}N_3O_5V$: C, 53.61; H, 3.50; N, 10.42%). IR (KBr, ν_{max}): 1598, 1573 (C=$N_{azomethine}$, C=N_{ring}), 1258 (C–$O_{enolate}$), 1048 (N–N), 956 cm^{-1} (V=O). Data for **10**: Yield 0.21 g (55%). (Found: C, 52.53; H, 3.65; N, 13.12. Calc. for $C_{19}H_{16}N_4O_5V$: C, 52.91; H, 3.74; N, 12.99%). IR (KBr, ν_{max}): 1600, 1583 (C=$N_{azomethine}$, C=N_{ring}), 1227 (C–$O_{enolate}$), 1047 (N–N), 964 cm^{-1} (V=O).

Organism culture conditions and *in vitro* testing against *E. histolytica*

The ligands, their metal complexes **2** and **7**, and [VO(acac)$_2$] were screened *in vitro* for antiamoebic activity against an HM1:1MSS strain of *E. histolytica* by the microdilution method.[27] *E. histolytica* trophozoites were cultured in TYIS-33 growth media as described previously in wells of 96-well microtiter plate (Coster).[28] All of the compounds (*ca.* 1 mg) were dissolved in DMSO (40 μL), and stock solutions were prepared freshly before use, adding enough culture medium to obtain a concentration of 1 mg mL^{-1}. Dissolution of the compounds was facilitated by mild sonication in a sonicleaner bath for a few minutes. As evident from the UV/Vis spectra of the complexes dissolved in DMSO and DMSO + TYIS-33 medium, the complexes preserve their integrity under test conditions and are stable.[29,30] Twofold serial dilutions were carried out in the wells of the 96-well microtiter plate in 170 μL of medium. Each test included metronidazole as a standard amoebicidal drug, control wells (culture medium plus amoebae) and a blank (culture medium

only). The control wells were prepared from a confluent culture by pouring off the medium, adding 2 mL of fresh medium, and chilling the culture on ice to detach the organisms from the flask wall. The number of amoeba per mL was estimated with a heamocytometer, and trypan blue exclusion was used to confirm viability. The cell suspension used was diluted to 10^5 organisms mL^{-1} by adding fresh culture medium, and 170 μL of this suspension was added to the test and control wells so that the wells were completely filled (total volume 340 μL). An inoculum of 1.7×10^4 organisms per well was chosen so that confluent but not excessive growth took place in the control wells. The plates were sealed with expanded polystyrene, secured with tape, placed in a modular incubation chamber and gassed for 10 min with nitrogen before incubation at 37 °C for 72 h.

Assessment of anti-amoebic activity

After incubation, the growth of amoebae in the plate was checked with a low power microscope. The culture medium was removed by inverting the plate and shaking gently. The plate was then immediately washed once in sodium chloride solution (0.9%) at 37 °C. This procedure was completed quickly, and the plate was not allowed to cool in order to prevent the detachment of amoebae. The plate was allowed to dry at room temperature, and the amoebae were fixed with methanol and, when dry, stained with 0.5% aqueous eosin for 15 min. Stained plates were washed once with tap water and then twice with distilled water and allowed to dry. A 200 μL portion of 0.1 N sodium hydroxide solution was added to each well to dissolve the protein and release the dye. The optical density of the resulting solution in each well was determined at 490 nm with a microplate reader. The % inhibition of amoebal growth was calculated from the optical densities of the control and test wells and plotted against the logarithm of the dose of the drug tested. Linear regression analysis was used to determine the best-fitting straight line from which the IC_{50} value was found. The significance of the statistical difference between the IC_{50} values of metronidazole and the active compounds **2** and **7** was established by the t-test.

Catalytic reactions

Oxidation of styrene. Oxidation of styrene was carried out with [{VO(acpy-nah)}$_2$(μ-O)$_2$] (**2**) and [{VO(acpy-fah)}$_2$(μ-O)$_2$] (**7**) as catalysts. In a typical reaction, styrene (1.04 g, 10 mmol) and aqueous 30% H_2O_2 (1.13 g, 10 mmol) were mixed in 10 mL of acetonitrile and the reaction mixture was heated with stirring to 80 °C. The catalyst (20 mg) was added to the reaction mixture and progress of the reaction was monitored by withdrawing reaction samples at different time intervals and analysing them quantitatively by gas chromatography.

Oxidation of ethyl benzene. Complexes **2** and **7** were also used to carry out the oxidation of ethylbenzene. Ethylbenzene (1.06 g, 10 mmol), aqueous 30% H_2O_2 (1.13 g, 10 mmol) and catalyst (20 mg) were transferred into acetonitrile (10 mL) and the reaction mixture was heated to 80 °C with stirring in an oil bath. The reaction products were analysed as mentioned above.

Results and discussion

Synthesis and solid state characteristics of the complexes

Scheme 2 provides an overview of the complexes reported in this contribution. Structures of these complexes are based on elemental analyses, spectroscopic (IR, UV/Vis, EPR, ^{1}H and ^{51}V NMR) data, electrochemical and thermogravimetric studies, and X-ray diffraction analyses of complexes **2** and **7**. The preparation of complexes **6** and **7** (the latter in a mixture with the dioxo complex [VO_2(acpy-fah)]) has been reported previously.[26] Ligands **I** and **II** coordinate through their enolate tautomeric form, *i.e.* the ONN(1−) mode, in these complexes; *cf.* Scheme 1.

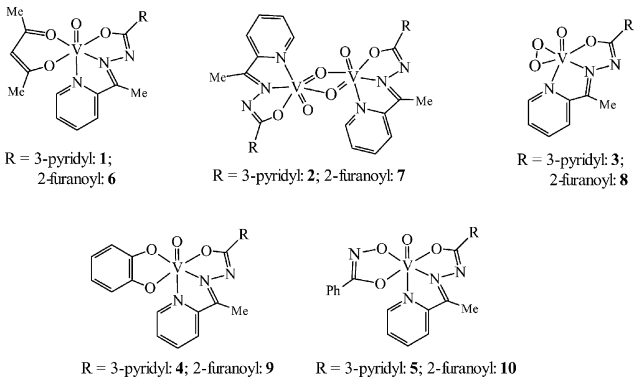

Scheme 2

A solution of [VO(acac)$_2$] reacted with Hacpy-nah (**I**) in refluxing methanol under anaerobic conditions, yielding the oxovanadium(IV) complex, [VO(acac)(acpy-nah)] (**1**). The stability of **1** is fair in the solid state, but **1** slowly converts to the μ-bis(oxo)bis{oxovanadium(V)} complex [{VO(acpy-nah)}$_2$(μ-O)$_2$] (**2**) on aerobic oxidation in methanol. For the direct preparation of **2**, the suspension of **1** in methanol can be oxidised directly. Eqns (1) and (2) represent the synthetic procedures.

$$\underset{\mathbf{I}}{[V^{IV}O(acac)_2] + \text{Hacpy-nah}} \rightarrow \underset{\mathbf{1}}{[V^{IV}O(acac)(acpy\text{-}nah)]} + \text{Hacac} \quad (1)$$

$$\underset{\mathbf{1}}{2[V^{IV}O(acac)(acpy\text{-}nah)]} + \tfrac{1}{2}O_2 + H_2O \rightarrow \underset{\mathbf{2}}{[\{VO(acpy\text{-}nah)\}_2(\mu\text{-}O)_2]} + 2\text{Hacac} \quad (2)$$

The corresponding furanoyl (acpy-fah) complexes **6** and **7** have been prepared accordingly (see also ref. 26). Complexes **2** and **7** can also be isolated from the reaction of vanadate, prepared *in situ* by stirring V_2O_5 in aqueous KOH, with the potassium salt of **I** or **II**, and adjusting the pH to *ca.* ~7, eqn (3).

$$\underset{\mathbf{II}}{2HV^{V}O_4^{2-} + 2\text{Hacpy-fah} + 4H^+} \rightarrow \underset{\mathbf{7}}{[\{V^{V}O(acpy\text{-}fah)\}_2(\mu\text{-}O)_2]} + 4H_2O \quad (3)$$

Complexes **1** and **6** serve as good starting materials for other oxovanadium(v) complexes. Thus, addition of the oxidant H_2O_2 to **1** or **6** yields the oxoperoxo vanadium(v) complexes **3** or **8**, as shown by eqn (4).

$$\underset{1}{2[V^{IV}O(acac)(acpy\text{-}nah)]} + 3H_2O_2 \rightarrow \underset{3}{2[V^{V}O(O_2)(acpy\text{-}nah)]} + 2Hacac + 2H_2O \quad (4)$$

Reaction of **1** and **6** with catechol or benzohydroxamic acid in methanol under aerobic conditions results in the formation of the mixed chelate oxovanadium(v) complexes **4**, **5**, **9** and **10**, as exemplified for **4** and **10** by eqns (5) and (6).

$$\underset{1}{[V^{IV}O(acac)(acpy\text{-}nah)]} + H_2cat + \tfrac{1}{2}O_2 + 2H^+ \rightarrow \underset{4}{2[V^{V}O(cat)(acpy\text{-}nah)]} + 2Hacac + H_2O \quad (5)$$

$$\underset{6}{[V^{IV}O(acac)(acpy\text{-}fah)]} + H_2bha + \tfrac{1}{2}O_2 + 2H^+ \rightarrow \underset{10}{2[V^{V}O(bha)(acpy\text{-}fah)]} + 2Hacac + H_2O \quad (6)$$

The paramagnetic complexes **1** and **6** exhibit a magnetic moment of 1.70 and 1.78 BM, respectively, while the other complexes are diamagnetic as expected for a $3d^0$ system. All complexes are soluble in methanol, ethanol, acetonitrile, DMF and DMSO.

TGA studies

The TGA profiles of the dinuclear complexes **2** and **7** show that they are stable up to *ca.* 210 °C but decompose in two steps on further increasing the temperature. The first mass loss of 40.8% in **2** and 35.3% in **7** occurs in the wide temperature range of 210–460 °C, followed by a mass loss of 31.4 and 35.4%, respectively, in a narrow temperature range of 460–510 °C. The total mass loss of 72.2% in **2** and 70.7% in **7** corresponds to the loss of all organic moieties minus half an oxygen (Calc. mass loss 71.7% for **2** and 70.4% for **7**). The remaining residues correspond to the formation of V_2O_5 (for **2**: obs. = 27.8, calc. = 28.3%; for **7**: obs. = 28.5, calc. = 29.3%). The mixed ligand complexes **1**, **4**, **5**, **6**, **9** and **10** lose weight in the temperature range of *ca.* 170–210 °C, corresponding to the loss of acac, cat or bha, minus one oxygen atom. This pattern is similar to the one observed earlier.[31] The resulting product apparently is a dioxo complex (see eqn 7) for **1**. On further heating, this intermediate decomposes following the above pattern to give V_2O_5 as the end product.

$$[VO(acac)(acpy\text{-}nah)] \rightarrow [VO_2(acpy\text{-}nah)] + \{(acac) - O\} \quad (7)$$

Structure descriptions

Selected bond distances and angles are provided in Table 1. Fig. 1 shows the molecular structure of **2**·1.5H_2O. The dinuclear molecules, containing the $\{O{=}V(\mu\text{-}O)\}_2$ core, are centrosymmetric. The μ-O bridge is asymmetric, with a short bond $d(V{=}O)$ = 1.66 Å (*i.e.* somewhat widened with respect to the terminal $d(V{=}O)$), and a rather long distance of *ca.* 2.3 Å to the second vanadium centre and *trans* to the terminal oxo group. Each vanadium centre is octahedrally coordinated, with O1=V-μ-O2 forming the almost linear axis. The vanadium centre is in the plane spanned by the three coordinating ligand functions (N1, N2, O3) and the symmetry-related bridging oxygen O2A. All of the vanadium–ligand and interligand structural parameters compare to what is found in related vanadium complexes with the rare asymmetrically bridged $\{O{=}V(\mu\text{-}O)\}_2$ core.[32–34] Compound **2** also contains 1.5 waters of crystallisation. Each water is disordered over three positions. The water molecules are in H-bonding contact with the N4 of the dangling pyridine at an average distance of 2.52 Å, and with neighbouring water molecules, forming pairs of pairs in a linear zigzag arrangement with average distances of 2.44 and 2.54 Å within and between pairs, respectively. These linear clusters consisting of 3.5 water molecules link two adjacent vanadium complexes.

Table 1 Selected bond lengths and angles for **2**

	2[a]
V1–O1	1.6158(10) Å
V1–O2	2.3022(9) Å
V1–O2A	1.6687(9) Å
V1–O3	1.9695(10) Å
V1–N1	2.1078(11) Å
V1–N2	2.1239(11) Å
V1 ··· V1A	3.120 Å
O1–V1–O2	175.04(5)°
O1–V1–O2A	106.00(5)°
V1–O2–V1A	102.41(4)°
O2–V1–O2A	77.59(4)°
O2A–V1–O3	105.77(5)°
O2A–V1–N2	152.45(4)°
O3–V1–N2	74.18(4)°
N1–V1–N2	73.22(4)°

[a] Symmetry operations used to generate the equivalent atoms V1A and O2A: $-x+\frac{1}{2}, -y+\frac{1}{2}, -z$.

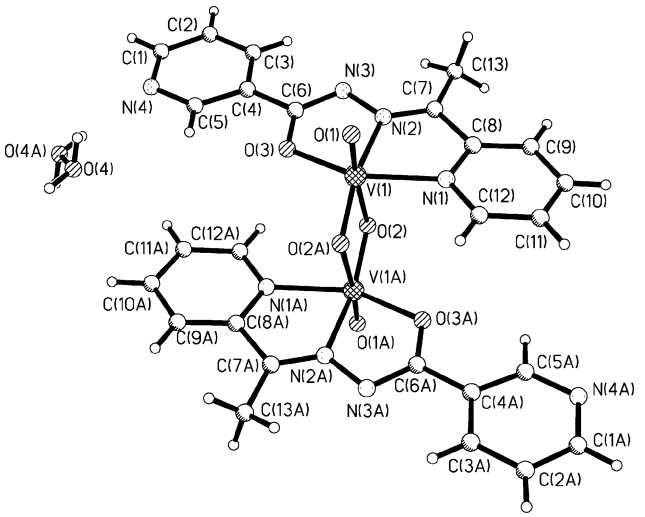

Fig. 1 ORTEP[55] plot (30% probability level) of **2**·1.5H_2O.

IR spectra

The IR spectra of the ligands exhibit two bands at 3191 and 1669 cm^{-1} (Hacpy-nah **I**), and at 3180 and 1678 cm^{-1}

(Hacpy-fah **II**) due to ν(NH) and ν(C=O) stretches, respectively. This is indicative of their ketonic nature in the solid state (*cf.* Scheme 1, left). The absence of these bands in the spectra of all of the complexes is consistent with the restructuring of the carbonyl moiety due to enolisation and subsequent proton replacement by the metal ion. A new band appearing in the region 1227–1277 cm^{-1} is assigned to the ($C–O_{enolic}$) mode. Both of the ligands display one or two sharp bands and one weak band in the 1580–1619 cm^{-1} region. Generally, $\nu(C=N_{azomethine})$ and ν(C=C) stretches appear as sharp bands, and $\nu(C=N_{ring})$ as a weak band. However, unequivocal assignment of these bands could not be made due to the complexity in this region, encompassing bands associated with coordinated azomethine and ring nitrogens, as documented by, *e.g.*, the complexes $[VO_2(pic\text{-}nah)]_2$,[32] $[VO_2(acpy\text{-}inh)]$ and $[VO_2(acpy\text{-}bhz)]$,[31] $[VO_2(acpy\text{-}sbdt)]$[16a] and in the complexes **2** and **7** reported here. A ligand band appearing at 990 cm^{-1} (in **I**) and at 1009 cm^{-1} (in **II**) due to ν(N–N) mode undergoes a shift to higher wave number by 15–42 cm^{-1} upon complex formation. This shift falls within the range commonly observed for monodentate coordination of the >N–N< residue. The high frequency shift of the ν(N–N) band on coordination is expected because of diminished repulsion between the lone pairs of adjacent nitrogen atoms.[35] The absence of the band corresponding to the ν(NH) and ν(OH) stretches of benzohydroxamic acid (Hbha) in complexes **5** and **10** is indicative of the enolate coordination mode of the ligand. The catecholate complexes **4** and **9** lack the ν(OH) and thus confirm the coordination of catecholate to the metal ion.

All of the complexes exhibit a strong band at 945–965 cm^{-1} due to the ν(V=O) mode, while the dioxo complexes display an additional band at 773–778 cm^{-1} due to the weakened ν(V=O) stretch as a result of the [V-(μ-O)-V] interaction. The peroxo complexes **3** and **8** show three IR active vibration modes associated with the peroxo moiety $\{V(O_2)^{3+}\}$ at 925–926, 773–775 and 593–594 cm^{-1}, which are assigned to the O–O intra-stretch (ν_1), the asymmetric $V(O_2)$ stretch (ν_3), and the symmetric $V(O_2)$ stretch (ν_2). The presence of these bands confirms the common η^2-coordination of the peroxo group.[36] In addition, these complexes exhibit an intense ν(V=O) at 963 (**3**) and 965 cm^{-1} (**8**).

Electronic spectra

The UV/Vis spectroscopic data of the ligands and complexes are presented in Table 2. The UV spectrum of Hacpy-nah (**I**) exhibits three absorption bands at 213, 294 and 362 nm, while the corresponding bands for Hacpy-fah (**II**) appear at 211, 304 and 362 nm. A weak shoulder between the first and second band is possibly due to H-bonding.[37] This band disappears on complexation. As most vanadium complexes exhibit a ligand to metal charge transfer transition (LMCT) band at *ca.* 400 nm, *i.e.* in the region where the third band appears, these two bands merge and appear as a broad band in the complexes. In addition, oxovanadium(IV) complexes display a weak band at 492 (**1**) or 522 nm (**6**) at high concentrations, which corresponds to a d-d band. Coordinated benzhydroxamate and catecholate induce strong charge transfer to the metal centre in complexes with high valency metal ions. Thus, a strong band at 550 nm for **5** and **10** and two intense bands at 518 and *ca.* 775 nm for **4** and **9** are assigned to LMCT originating from lone pair of p-orbitals on the hydroxamato[38] and catecholato[39] oxygen atom, respectively, into an empty d orbital of the vanadium ion.

^{1}H NMR spectra

The coordination modes of the ligands were further confirmed by recording ^{1}H NMR spectra of the ligands and complexes. Table 3 contains the spectral data. Both ligands exhibit a medium intensity signal at 11.13 (**I**) and 10.75 (**II**) due to the NH proton of the hydrazone moiety. As expected, this signal is absent in the complexes. The aromatic protons of the ligands as well as complexes appear well within the expected range. Aromatic protons of the coordinated catecholate (in **4** and **9**) appear at 6.61

Table 2 Electronic spectral data

Complex	Wavelength/nm (ε/M^{-1} cm^{-1})
Hacpy-nah	213(16 631), 294(21 006), 362(15 477)
[VO)(acac)(acpy-nah]	209(15 726), 285(15 438), 384(5078)
$[\{VO(acpy\text{-}nah)\}_2(\mu\text{-}O)_2]$	274(13 113), 382(9093)
[VO(cat)(acpy-nah)]	251(19 781), 263(19 791), 384(14 808), 517(4568), 789(4646)
[VO)(bha)(acpy-nah]	254(10 709), 287(10 168), 388(4199), 529(725)
Hacpy-fah	211(7943), 256(7883), 304(15 266), 362(3722)
[VO(acac)(acpy-fah)]	211(19 418), 290(14 310), 387(4915)
$[\{VO(acpy\text{-}fah)\}_2(\mu\text{-}O)_2]$	224(4280), 261(4388), 310(5747), 398(1001)
[VO(cat)(acpy-fah)]	269(20 511), 300(20 311), 395(9224), 524(2062), 784(2072)
[VO(bha)(acpy-fah)]	256(20 360), 295(18 510), 398(11 401), 530(2158)

Table 3 ^{1}H NMR spectral data of ligands and complexes

Complex	-NH	$-CH_3$	Aromatic
Hacpy-nah	11.13(s, 1H)	2.50(s, 3H)	7.48–9.12(m, 8H)
$[\{VO(acpy\text{-}nah)\}_2(\mu\text{-}O)_2]$		2.70(s, 3H)	6.75–8.81(m, 8H)
[VO(cat)(acpy-nah)]		2.78(s, 3H)	6.61(m, 2H), 6.72(m, 2H), 7.58–9.19(m, 8H)
[VO(bha)(acpy-nah)]		2.72(s, 3H)	7.32–9.96(m, 13H)
Hacpy-fah	10.75(s, 1H)	2.50(s, 3H)	6.88–8.67(m, 7H)
$[\{VO(acpy\text{-}fah)\}_2(\mu\text{-}O)_2]$		2.79(s, 3H)	7.55–9.23(m, 7H)
[VO(cat)(acpy-fah)]		2.72(s ,3H)	6.61(m, 2H), 6.72(m, 2H), 7.28–8.80(m, 7H)
[VO(bha)(acpy-fah)]		2.71(s, 3H)	6.72–8.83(m, 12H)

and 6.72 as multiplets, while those of benzohydroxamate (in **5** and **10**) appear in the aromatic regions, thus making this region rather complex.

^{51}V NMR and EPR spectra

The ^{51}V NMR spectral data of complexes **2**, **4**, **5**, **7**, **9** and **10** are collated in Table 4. The binuclear complexes **2** and **7** exhibit one strong resonance at −509.3 (**2**) or −508.2 ppm (**7**), which is well within the range expected for the vanadium(V) complexes having a mixed O/N donor set.[40,41] The catecholate complexes **4** and **9** display two bands: the low field signal at +343 ppm (**4**) and +340 ppm (**9**) reflects the effective charge transfer from the non-innocent catecholate ligand to the vanadium(V) centre[39] and thus belongs to the mixed ligand complexes [VO(cat)L], whereas the high field signal at −506.9 (**4**) and −513.5 (**9**) ppm belongs to a dioxovanadium species—apparently formed by partial decomposition—without direct coordination of catecholate. The intensity of the band assigned to the decomposition product increases with time at the extent of the catecholato complex (see also the UV/Vis section). The ^{51}V NMR spectra of **2** and **4** are compared in Fig. 2. Similarly, **5** and **10** display two bands at +66.5 and −502.9 ppm (**5**), and at +58.5 and −505.7 ppm (**10**). The low-field resonances represent the benzohydroxamato complexes **5** and **10**, where the hydroxymate induces the low field shift due to LMCT.[42] The high field signal belongs to the corresponding binuclear species. A slight deviation in peak 1 with respect to

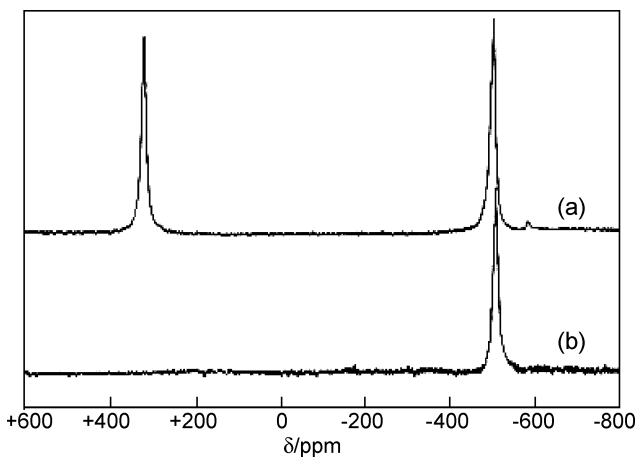

Fig. 2 ^{51}V NMR spectra of **2** (b, below) and **4** (a, above) recorded in DMSO-d_6 45 min after dissolution.

Table 4 ^{51}V NMR spectral data

Complex	Chemical shift (δ)/ppm Peak 1	Peak 2
[{VO(acpy-nah)}$_2$(μ-O)$_2$], **2**	−509.3	
[VO(cat)(acpy-nah)], **4**	−506.9	343
[VO(bha)(acpy-nah)], **5**	−502.9	66.5
[{VO(acpy-fah)}$_2$(μ-O)$_2$], **7**	−508.2	
[VO(cat)(acpy-fah)], **9**	−513.5	340
[VO(bha)(acpy-fah)], **10**	−505.7	58.5

Table 5 EPR data

Complex	g_0	$g_{x,y}g_z$	$A_0/\times 10^{-4}$ cm^{-1}	$A_{x,y},A_z/\times 10^{-4}$ cm^{-1}
1	1.971	1.98, 1.95	94	60, 168
6	1.97	1.98, 1.95	93	60, 165

solutions containing authentic **2** and **7** is a medium effect, imparted by the presence of catechol/benzohydroxamic acid.

EPR spectra have been obtained for the paramagnetic VO^{2+} complexes [VO(acaca)(acpy-nah)] (**1**) and [VO(acac)(acpy-fah)] (**6**) in DMSO at room temperature and 100 K (Table 5). The spectra exhibit the common eight line (isotropic) and 2 × 8 line patterns (nonrhombic anisotropic). The parallel component of the hyperfine coupling constant, A_z = 168 (**1**) and 165 × 10^{-4} cm^{-1} (**6**) correspond to the expected one calculated from the partial contributions of an equatorial NO_3 donor set, where N is an imine nitrogen, two O functions are from the acac(1-) ligand and the third oxygen is an alcoholate/enolate O.[43,44]

Electrochemical study

The oxovanadium(IV) complexes **1** and **6** are easily oxidisable in solution under aerobic conditions (see Experimental). Their irreversible oxidation has also been noticed by cyclic voltammetry. Thus, complexes **1** and **6** exhibit an irreversible sharp oxidation peak at −700 mV. In contrast, the dioxovanadium(V) complexes **2** and **7** display quasi-reversible reduction–oxidation at a midpoint potential of −637 mV for **2** and −750 mV for **7**, corresponding to the V^{V}–V^{VI} couple.[45] In addition, there is an essentially irreversible reduction at E_{pc} = −1250 (**2**) and −1809 V (**7**). No appreciable change in CV was noted when recording the voltammogram of **2** at two different scan rates, *viz.* 50 and 200 mV s^{-1}.

Reactivity studies

Complexes **4**, **5**, **9** and **10** are stable in dry CH_2Cl_2 and acetonitrile for several days and about two days in methanol but they slowly decompose in DMF and DMSO, as already shown by ^{51}V NMR spectroscopy, into dioxo complexes. The decomposition of the VO^{3+} complexes **4** and **9** into VO_2^+ species with the loss of the bidentate catecholate (2-) was also monitored spectrophotometrically in DMSO (Fig. 3). This conversion is rather slow in dry solvent and takes about 24 h, while addition of a few drops of water facilitates decomposition, leading to completion within about 3 h. During this process, a gradual loss in intensity of the LMCT bands originating from coordinated catecholate and finally their disappearance was observed. The bands appearing at *ca.* 385 and 265 nm experienced only marginal shifts towards lower energy. The suggested reaction is represented by eqn (8), taking into account that the primary decomposition products of the catecholate or benzohydroxamate complexes should be mononuclear species.

$$[VO(cat)L] + H_2O \rightarrow [VO_2L] + H_2cat \quad (8)$$

Addition of a small amount of L-ascorbic acid to the DMSO solution of **4** or **9** (1 mL of *ca.* 10^{-1} M solution of L-ascorbic acid in 9 mL of 10^{-4} solution of **4** or **9**) reduces the decomposition time to about 20 min. As oxovanadium(V) complexes generally undergo

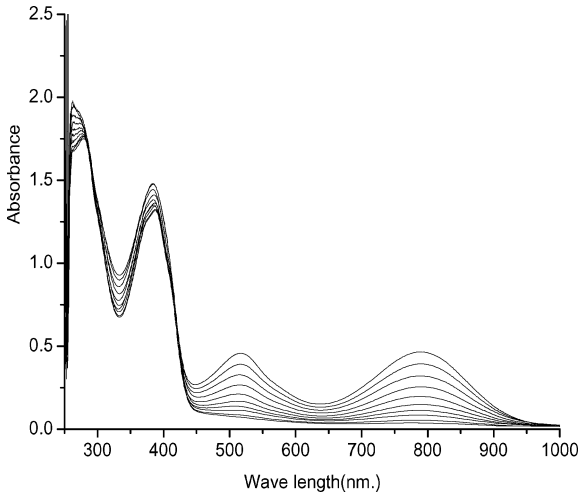

Fig. 3 Decomposition of [VO(cat)(acpy-nah)] (**4**) in 5 mL of DMSO after the addition of two drops of water, as a function of time.

redox reactions with reducing agents such as ascorbic acid, the reaction path observed here possibly reflects reduction of **4** and **9** with concomitant removal of coordinated catecholate, followed by rapid reoxidation of the reduced species to form the dioxo complex $[VO_2L]$. The L-ascorbic acid is thus simply working as a mediator in electron transfer.

Dioxovanadium(V) complexes are known to react with acids to give hydroxo(oxo) complexes (*vide infra*), and the corresponding hydroxo(oxo) species has also been generated from [{VO(acpy-fah)}$_2$(μ-O$_2$)] (**7**) on reaction with HCl. Dropwise addition of HCl-saturated methanol to a methanolic solution of **7** causes darkening of the solution with a gradual shift of the 398 nm band, along with a slight broadening and decrease in intensity of the absorption maximum (Fig. 4). At the same time, the UV band at 310 nm shifts to 328 nm along with an increase in intensity, while the 261 and 224 nm bands remain nearly unchanged. We interpret this result in terms of the formation of the complex [VO(OH)(Hacpy-fah)]$^{2+}$ *via* [VO$_2$(Hacpy-fah)]$^+$, with one of the >N–N< nitrogens being the site of protonation, as shown by eqns (9) and (10)

$$[\{VO(acpy\text{-}fah)\}_2(\mu\text{-}O_2)] + 2H^+ \rightarrow 2[VO_2(Hacpy\text{-}fah)]^+ \quad (9)$$

$$[VO_2(Hacpy\text{-}fah)]^+ + H^+ \rightarrow [VO(OH)(Hacpy\text{-}fah)]^{2+} \quad (10)$$

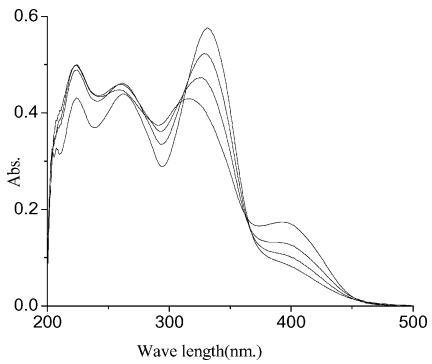

Fig. 4 Titration of [{VO(acpy-fah)}$_2$(μ-O$_2$)] (**7**) with a saturated solution of HCl in methanol; spectra were recorded after the dropwise addition of MeOH–HCl to 10 mL of *ca.* 10^{-4} M MeOH solution of **7**.

A protonated dioxo complex with the hydrazide N as the site of protonation has been structurally characterized in the case of [VO$_2$(Hsal-bhz)] (where H$_2$sal-bhz is the hydrazone derived from salicylaldehyde and benzoylhydrazide),[46] while [VO$_2$(Hsal-nah)] and [VO$_2$(Hsal-fah)] (H$_2$sal-nah and H$_2$sal-fah are derived from salicylaldehyde and nicotinic acid hydrazide or 2-furoic acid hydrazide) have been established by spectroscopic studies.[47]

Hydroxo(oxo)vanadium complexes have previously also been generated on the acidification of K[VO$_2$(sal-inh)H$_2$O][48] (H$_2$sal-inh = hydrazone derived from salicylaldehyde and isonicotinic acide hydrazide) and [K(H$_2$O)$_2$][VO$_2$(Clsal-sbdt)][16a] (H$_2$Clsal-sbdt = ligand derived from 5-chlorosalicylaldehyde and S-benzyldithiocarbazate). A hydroxo(oxo) complex, [VO(OH)(LH)]$^+$ (where LH = N-[{(*o*-hydroxyphenyl)methyl}-N′-(2-hydroxyethyl)ethylenediamine) has been reported to form in solution from a binuclear dioxovanadium(V) precursor in a similar manner.[49] [V^{V}O(OH)(8-oxyquinolinate)$_2$][50] and [V^{IV}O(OH)Tp(H$_2$O)][51] [Tp = *tris*(3,5-diisopropyl-1-pyrazolyl)-borate(1-)] have been characterised in the solid state.

The solution acquired the original spectrum of **7** on addition of a methanolic solution of KOH to [VO(OH)(Hacpy-fah)]$^{2+}$, so the reaction is thus reversible. This reversibility is an important observation in the context of the active site structure and the catalytic activity of vanadate-dependent haloperoxidases, for which a hydroxo ligand at the vanadium centre has been proposed on the basis of X-ray diffraction data.[52]

Antiamoebic activity

The *in vitro* antiamoebic activities of the hydrazone based ligands **I** and **II** and their vanadium complexes **2** and **7** were carried out using the HM1:1MSS strain of *E. histolytica* to ascertain the effectiveness of metal complexes in comparison to their respective ligands. Table 6 presents the 50% inhibition concentration (IC_{50}) values in μM along with reference drug metronidazole (IC_{50} = 1.81 μM). The biological data suggests that the free ligands possess no activity against the trophozoites of *E. histolytica* (**I**: IC_{50} = 9.63 μM, **II**: IC_{50} = 8.68 μM) as compared to metronidazole, while complexes **2** (IC_{50} = 1.68 μM) and in particular **7** (IC_{50} = 0.45 μM) showed promising activity. The vanadium complexes precursor [VO(acac)$_2$], IC_{50} = 5.33 μM, was also considerably less active. Apparently the combination of vanadium and coordinated hydrazone provided the best results, suggesting the possibility of developing vanadium complexes based on hydrazone ligands as potential drug candidates for antiamoebic activity. The complexation reduces the polarity of the central metal atom because of partial sharing of its positive charge with the ligand, which favours permeation of

Table 6 *In vitro* antiamoebic activities of ligands and their vanadium complexes against (HM1:1MSS) strain of *E. histolytica*

Compound	IC_{50}/μM	S.D.[a]
Hacpy-nah **I**	9.63	0.10
Hacpy-fah **II**	8.68	0.13
[{VO(acpy-nah)}$_2$(μ-O)$_2$] **2**	1.68	0.16
[{VO(acpy-fah)}$_2$(μ-O)$_2$] **7**	0.45	0.06
[VO(acac)$_2$]	5.33	0.04
Metronidazole	1.8	0.31

[a] Standard deviation.

the complexes through the lipid layer of cell membrane.[53] The results were statistically evaluated by analysis of variance. The null hypothesis was tested using the t-test. The significance of the difference between the IC_{50} values of metronidazole and the complexes **2** and **7** was evaluated by the t-test. The values of the calculated t were found higher than the table value of t at 5% level which concludes that the complexes under study should significantly induced the treatment of amoebiasis.

Catalytic activity studies

The ability of these vanadium complexes to catalyse oxidation reaction have been studied with the complexes [{VO(acpy-nah)}$_2$(μ-O)$_2$] (2) and [{VO(acpy-fah)}$_2$(μ-O)$_2$] (**7**).

(i) Oxidation of styrene. Oxidation of styrene catalysed by **2** and **7** gave styrene epoxide, phenylacetaldehyde, benzaldehyde, benzoic acid and 1-phenyl-ethane-1,2-diol along with only minor amounts (less than 2%) of unidentified products. The oxidative conversion of styrene is somewhat dependent on the amount of oxidant (here H_2O_2) present. As shown in Fig. 5, at a molar ratio styrene : H_2O_2 = 1 : 1, 72% conversion was achieved in 6 h contact time with catalyst **2**. Increasing the ratio to 1 : 2 increases the conversion to 86.4%. This conversion goes down to 81.2% on further increasing the ratio to 1 : 3. The dilution of the reaction mixture due to the presence of larger amounts of water in the H_2O_2 may be a possible reason for the lower conversion. Complex **7** has a very similar catalytic activity; here, 75.4 and 84.0% conversions were achieved with 1 : 1 and 1 : 2 styrene : H_2O_2 ratios, respectively. However, the turnover rates per hour are comparable for the 1 : 1 and 1 : 2 cases. The differences in the product spectrum at different styrene : H_2O_2 molar ratios are shown in Table 7. Independent of the molar ratio, the amounts of products follow the order: benzaldehyde > 1-phenyl-ethane-1.2-diol > benzoic acid > styrene oxide > phenylacetaldehyde. No further conversion of styrene or change in selectivity was noticed beyond 6 h of reaction time.

The formation of styrene epoxide, an important intermediate for the manufacture of the perfumery chemical phenylethyl alcohol, is low. The styrene oxide formed in the first step by epoxidation is mainly converted into benzaldehyde *via* the intermediate hydroxyl-hydroperoxistyrene. Alternatively, benzaldehyde forms through direct oxidative cleavage of the styrene side chain double bond *via* a radical mechanism. Benzoic acid formation through benzaldehyde is rather slow in all reactions. Similarly, the amount of phenylacetaldehyde, a product formed by isomerisation of styrene oxide, is low in all cases. Water present in H_2O_2 is probably responsible for the hydrolysis of styrene oxide to form 1-phenyl-ethane-1,2-diol to some extent.[54] The formation of all these products is represented in Scheme 3

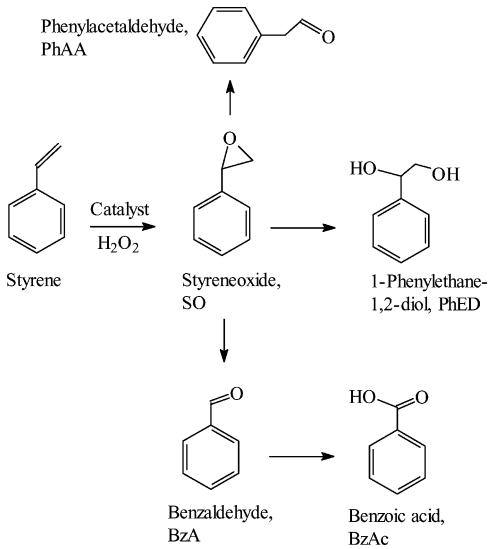

Scheme 3

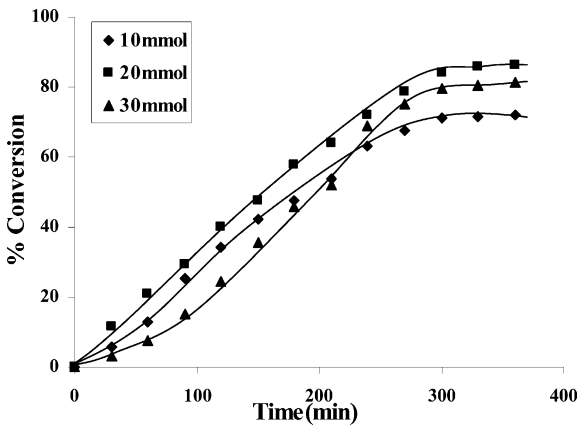

Fig. 5 Effect of the molar amounts of H_2O_2 on the conversion of styrene (1.04 g, 10 mmol) in CH_3CN (10 mL) at 80 °C in the presence of 20 mg of catalyst.

(ii) Oxidation of ethylbenzene. Complexes **2** and **7** also catalyse the oxidation of ethylbenzene to give benzyl alcohol, benzaldehyde and 1-phenyl-ethane-1.2-diol (Scheme 4).

Table 7 Effect of oxidant on percentage conversion of styrene and selectivity of various oxidation products after 6 h reaction time

				Product selectivity				
Catalyst	Substrate : H_2O_2	Conv. (%)	TOF/h^{-1}	SO[a]	PhAA[b]	BzA[c]	BzAc[d]	PhED[e]
[{VO(acpy-nah)}$_2$(μ-O)$_2$]	1 : 1	72.1	19.4	5.53	0.70	50.57	6.19	37.04
	1 : 2	86.4	23.2	5.15	0.44	58.01	9.60	26.78
	1 : 3	81.2	21.8	6.31	0.79	61.57	9.33	22.01
[{VO(acpy-fah)}$_2$(μ-O)$_2$]	1 : 1	75.36	19.6	4.01	0.88	60.85	5.69	28.56
	1 : 2	84.05	21.9	3.82	0.51	68.62	2.76	24.29
	1 : 3	79.28	20.7	4.46	0.72	75.02	3.36	16.44

[a] Styrene epoxide. [b] Phenylacetaldehyde. [c] Benzaldehyde. [d] Benzoic acid. [e] 1-Phenyl-ethane-1,2-diol.

Table 8 Effect of oxidant on percentage conversion of ethyl benzene and selectivity of various oxidation products

Catalyst	Substrate : H_2O_2	Conversion (%)	TOF/h^{-1}	Selectivity (%)		
				Benzyl alcohol	Benzaldehyde	1-Phenyl-ethane-1.2-diol
[{VO(acpy-nah)}$_2$(μ-O)$_2$]	1 : 1	20.82	5.6	73.46	13.62	12.91
	1 : 2	28.30	7.6	73.18	14.46	12.26
	1 : 3	30.16	8.1	79.85	14.11	6.04
[{VO(acpy-fah)}$_2$(μ-O)$_2$]	1 : 1	20.49	5.3	72.16	14.78	13.05
	1 : 2	85.93	22.4	80.79	8.66	10.55
	1 : 3	70.18	18.3	82.50	8.03	9.46

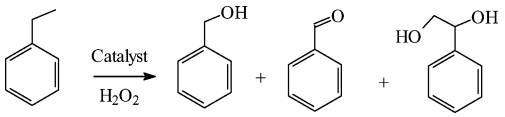

Scheme 4

Reaction conditions were optimised for the maximum oxidation by varying the amount of H_2O_2, and the effect is presented in Fig. 6. At a molar ratio ethylbenzene : H_2O_2 = 1 : 1, the reaction in the presence of the catalyst [{VO(acpy-nah)}$_2$(μ-O)$_2$] (**2**) proceeded slowly in the beginning and gave 20.8% conversion of ethyl benzene in 6 h contact time. Increasing the substrate : H_2O_2 molar ratio to 1 : 2 increases the conversion to 28.3% and reaches completion within 4 h, while further enhancement of H_2O_2 hardly affects the conversion. The catalyst [{VO(acpy-fah)}$_2$(μ-O)$_2$] (**7**) shows very similar results with a 1 : 1 ratio; the conversion level was raised to 85.9%, however, at a 1 : 2 ratio. Further increasing the ratio in favour of the oxidant again decreases conversion. Among the reaction products, benzyl alcohol is formed preferentially, followed by benzaldehyde and 1-phenyl-ethane-1,2-diol. Table 8 presents the results. We did not observe the formation of acetophenone under these reaction conditions.

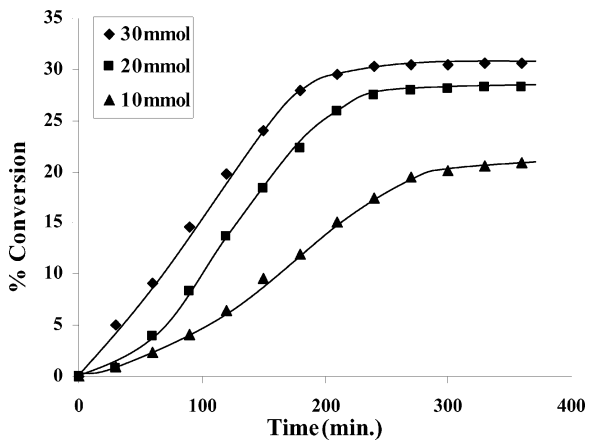

Fig. 6 Effect of H_2O_2 on the conversion of ethylbenzene. Conditions: ethylbenzene (1.06 g, 10 mmol), catalyst **2** (20 mg), CH_3CN (10 mL), temperature (80 °C).

Conclusion

Vanadylbis(acetylacetonate) [VO(acac)$_2$] reacts with hydrazone ligands based on acetylpyridine and the hydrazides of nicotinic or furoic acid, L, to yield oxovanadium(IV) complexes by the replacement of one of the acac(1-) by L(1-). These complexes are susceptible to aerobic oxidation, converting to binuclear dioxovanadium(V) complexes [{LVO(μ-O)}$_2$] (**2** and **7**) containing the rare *anti*-{O=V(μ-O)}$_2$ diamond core with asymmetrically bridging μ-O^{2-}. In the presence of catechol or benzhydroxamic acid, labile mixed ligand complexes with catecholate or hydroxamate along with the hydrazone are obtained, which exhibit uncommon low field shifts of their ^{51}V resonances due to their non-innocent nature. Compounds **2** and **7** can be reversibly protonated with HCl in methanolic solution to the hydroxo-oxo complexes [HLVO(OH)]$^{2+}$, modelling a possible intermediate state of vanadate-dependent haloperoxidases during turnover. **2** and **7** further model the oxo-transfer activity of these enzymes in as far as they catalyse the conversion, by H_2O_2, of styrene and ethylbenzene to benzaldehyde, benzoic acid and 1-phenyl-ethane-1,2-diol. Both complexes also show antiamoebic activity comparable to (**2**) or better than (**7**) the commonly used amoebicidal drug metronidazole. No such activity is observed with [VO(acac)$_2$] or the uncomplexed hydrazone ligands.

Acknowledgements

We acknowledge performance of the microanalyses by the Sophisticated Analytical Instrumental Facility, CDRI, Lucknow, and financial assistance from the Department of Science and Technology, Government of India (Grant No. SP/S1/F-07/2001), New Delhi, and the Deutsche Forschungsgemeinschaft (grant RE 431/20–1).

References

1 (*a*) E. J. Barreiro, C. A. M. Fraga, A. L. P. Miranda and C. R. Rodrigues, *Quim. Nova*, 2002, **25**, 129; (*b*) A. R. Todeschini, A. L. P. Miranda, K. C. M. Silva, S. C. Parrini and E. J. Barreiro, *Eur. J. Med. Chem.*, 1998, **33**, 189; (*c*) A. C. Cunha, J. M. Figueiredo, J. L. M. Tributino, A. L. P. Miranda, H. C. Castro, R. B. Zingali, C. A. M. Fraga, M. C. B. V. Souza, V. F. Ferreira and E. J. Barreiro, *Bioorg. Med. Chem.*, 2003, **11**, 2051.
2 J. P. Mahy, S. Gaspard and D. Mansuy, *Biochemistry*, 1993, **32**, 4014.
3 M. R. Maurya, *Coord. Chem. Rev.*, 2003, **237**, 163.
4 (*a*) A. Butler, *Coord. Chem. Rev.*, 1999, **187**, 17; (*b*) M. Weyand, H. J. Hecht, M. Kieβ, M. F. Liaud, H. Vilter and D. Schomburg, *J. Mol. Biol.*, 1999, **293**, 595; (*c*) M. I. Isupov, A. R. Dalby, A. A. Brindley, Y. Izumi, T. Tanabe, G. N. Murshudov and J. A. Littlechild, *J. Mol. Biol.*, 2000, **299**, 1035; (*d*) G. J. Colpas, B. J. Hamstra, J. W. Kampf and V. L. Pecoraro, *J. Am. Chem. Soc.*, 1996, **118**, 3469; (*e*) B. J. Hamstra, G. J. Colpas and V. L. Pecoraro, *Inorg. Chem.*, 1998, **37**, 949; (*f*) J. A. Littlechild and E. Garcia-Rodriguez, *Coord. Chem. Rev.*, 2003, **237**, 65; (*g*) S. Macedo-Ribeiro, W. Hemrika, R. Renirie, R. Wever and A. Messerschmidt, *JBIC, J. Biol. Inorg. Chem.*, 1999, **4**, 209; (*h*) A. Messerschmidt and R. Wever, *Proc. Natl. Acad. Sci. U. S. A.*, 1996, **93**, 392.
5 D. Rehder, *Inorg. Biochem.*, 2000, **80**, 133.

6 A. A. Antipov, D. Y. Sorokin, N. P. L'Vov and J. G. Kuenen, *Biochem. J.*, 2003, **369**, 185.
7 R. E. Berry, E. M. Armstrong, R. L. Beddoes, D. Collison, S. N. Ertok, M. Helliwell and C. D. Garner, *Angew. Chem., Int. Ed.*, 1999, **38**, 795.
8 (*a*) D. L. Parry, S. G. Brand and K. Kustin, *Bull. Mar. Sci.*, 1992, **50**, 302; (*b*) T. Ishii, I. Nakai, C. Numako, K. Okoshi and T. Otake, *Naturwissenschaften*, 1993, **80**, 268.
9 M. J. Gresser, A. S. Tracey, in *Vanadium in Biological Systems*, ed. N. D. Chasteen, Kluwer Academic Publishers, Dordrecht, 1990, ch. IV.
10 (*a*) K. H. Thompson, J. H. McNeil and C. Orvig, *Chem. Rev.*, 1999, **99**, 2561; (*b*) K. H. Thompson and C. Orvig, *Coord. Chem. Rev.*, 2001, **1033**, 219; (*c*) M. Melchior, K. H. Thompson, J. M. Jong, S. J. Retting, E. Shuter, V. G. Yuen, Y. Zhou, J. H. McNeil and C. Orvig, *Inorg. Chem.*, 1999, **38**, 2288; (*d*) B. A. Reul, S. S. Amin, J.-P. Buchet, L. N. Ongemba, D. C. Crans and S. M. Brichard, *Br. J. Pharmacol.*, 1999, **126**, 467; (*e*) S. S. Amin, K. Cryer, B. Zhang, S. K. Dutta, S. S. Eaton, O. P. Anderson, S. S. Miller, B. A. Reul, S. M. Brichard and D. C. Crans, *Inorg. Chem.*, 2000, **39**, 406; (*f*) D. C. Crans, *J. Inorg. Biochem.*, 2000, **80**, 123; (*g*) V. L. Pecoraro, C. Slebodnick, B. Hamstra, in *Vanadium Compounds: Chemistry, Biochemistry and Therapeutic Applications*, ed. D. C. Crans, A. S. Tracy, ACS Symposium Series 1998, ch. 12; (*h*) D. Rehder, *Inorg. Chem. Commun.*, 2003, **6**, 604; (*i*) H. Sakurai, Y. Kojima, Y. Yoshikawa, K. Kawabe and H. Yasui, *Coord. Chem. Rev.*, 2002, **226**, 187; (*j*) D. Rehder, J. Costa Pessoa, C. F. G. C. Geraldes, M. M. C. Castro, T. Kabanos, T. Kiss, B. Meier, G. Micera, L. Pettersson, M. Rangel, A. Salifoglou, I. Turel and D. Wang, *JBIC, J. Biol. Inorg. Chem.*, 2002, **7**, 384; (*k*) S. Takeshita, I. Kawamura, T. Yashuno, C. Kimura, T. Yamamoto, J. Seki, A. Tamura and H. Sakirai, *J. Inorg. Biochem.*, 2001, **85**, 179; (*l*) E. Kiss, K. Kawabe, A. Tamura, T. Jakusch, H. Sakurai and T. Kiss, *J. Inorg. Biochem.*, 2003, **95**, 69; (*m*) R. Shukla, V. Barve, S. Padhye and R. Bhonde, *Bioorg. Med. Chem.*, 2004, **14**, 4961; (*n*) M. Xie, L. Gao, L. Li, W. Liu and S. Yan, *J. Inorg. Biochem.*, 2005, **99**, 546.
11 M. Halberstam, N. Cohen, P. Slimovich, L. Rossetti and H. Shamoon, *Diabetes*, 1996, **45**, 659.
12 C. Orvig, K. H. Thompson, personal communication.
13 World Health Organisation, WHO/PAHO/UNESCO report of a consultation of experts on amoebiasis, *Weekly Epidemiological Record of the WHO*, 1997, 72, p. 97.
14 P. L. Johanson, *Parasitol. Today*, 1993, **9**, 183.
15 P. Goldman, R. L. Koch, T. C. Yeung, E. J. Chrystal, B. B. Beaulieu, Jr., M. A. McLafferty and G. Sudlow, *Biochem. Pharmacol.*, 1986, **35**, 43.
16 (*a*) M. R. Maurya, S. Khurana, Shailendra, A. Azam, W. Zhang and D. Rehder, *Eur. J. Inorg. Chem.*, 2003, 1966; (*b*) N. Bharti, Shailendra, M. T. Gonzalez Garza, D. E. Cruz-Vega, J. Castro-Garza, K. Saleem, F. Naqvi, M. R. Maurya and A. Azam, *Bioorg. Med. Chem. Lett.*, 2000, **12**, 869.
17 Y. Zhang and R. H. Holm, *Inorg. Chem.*, 1990, **29**, 911.
18 I. W. C. E. Arends, M. P. Birelli and R. A. Sheldon, *Stud. Surf. Sci. Catal.*, 1997, **110**, 1031.
19 H. B. ten Brink, H. E. Schoemaker and R. Wever, *Eur. J. Biochem.*, 2001, **268**, 132.
20 C. Bolm and F. Bienewald, *Angew. Chem., Int. Ed. Engl.*, 1995, **34**, 2640.
21 G. Santoni, G. M. Licini and D. Rehder, *Chem. –Eur. J.*, 2003, **9**, 4700.
22 T. S. Smith II and V. L. Pecoraro, *Inorg. Chem.*, 2002, **41**, 6750.
23 (*a*) V. Conte, F. D. Furia and G. Licini, *Appl. Catal., A*, 1997, **157**, 335; (*b*) A. G. J. Ligtenbarg, R. Hage and B. L. Feringa, *Coord. Chem. Rev.*, 2003, **237**, 89.
24 R. A. Row and M. M. Jones, *Inorg. Synth.*, 1957, **5**, 113.
25 R. L. Dutta and A. Syamal, *Elements of Magnetochemistry*, Affiliated East-West Press, New Delhi, 2nd edn, 1993, p. 8.
26 V. D. Deflon, D. M. de Oliveira, G. F. de Sousa, A. A. Batista, L. R. Dinelli and E. E. Castellano, *Z. Anorg. Allg. Chem.*, 2002, **628**, 1140.
27 C. W. Wright, M. J. O'Neill, J. D. Phillipson and D. C. Warhurst, *Antimicrob. Agents Chemother.*, 1988, **32**, 1725.
28 L. S. Diamond, D. R. Harlow and C. C. Cunnick, *Trans. R. Soc. Trop. Med. Hyg.*, 1978, **72**, 431.
29 F. D. Gillin, D. S. Reiner and M. Suffness, *Antimicrob. Agents Chemother.*, 1982, **22**, 342.
30 A. T. Keen, A. Harris, J. D. Phillipson and D. C. Warhurst, *Planta Med.*, 1986, 278.
31 M. R. Maurya, S. Khurana, W. Zhang and D. Rehder, *J. Chem. Soc., Dalton Trans.*, 2002, 3015.
32 S. Pal and S. Pal, *J. Chem. Crystallogr.*, 2000, **30**, 329.
33 X. Li, M. S. Lah and V. L. Pecoraro, *Inorg. Chem.*, 1988, **27**, 4657.
34 S. Meicheng, D. Xun and T. Youqi, *Sci. Sin., Ser. B (Engl. Ed.)*, 1988, **31**, 789.
35 S. P. Perlepes, D. Nicholls and M. R. Harison, *Inorg. Chim. Acta*, 1985, **102**, 137.
36 (*a*) A. D. Westland, F. Haque and J.-M. Bouchard, *Inorg. Chem.*, 1980, **19**, 2255; (*b*) M. Casný and D. Rehder, *Dalton Trans.*, 2004, 839; (*c*) M. Sivák, M. Mad'orová, J. Taatiersky and J. Marek, *Eur. J. Inorg. Chem.*, 2003, 2075.
37 A. T. T. Hsieh, R. M. Sheahan and B. O. West, *Aust. J. Chem.*, 1975, **28**, 885.
38 S. Gao, Z.-Q. Weng and S.-X. Liu, *Polyhedron*, 1998, **15**, 3595.
39 (*a*) G. Asgedom, A. Sreedhara and C. P. Rao, *Polyhedron*, 1996, **15**, 3731; (*b*) C. R. Cornman, J. Kampf and V. L. Pecoraro, *Inorg. Chem.*, 1992, **31**, 1981.
40 (*a*) D. Rehder, C. Weidemann, A. Duch and W. Priebsch, *Inorg. Chem.*, 1988, **27**, 584; (*b*) D. Rehder, in *Transition Metal Nuclear Magnetic Resonance*, ed. P. S. Pregosin, Elsevier, New York 1991, pp. 1–58.
41 O. W. Howarth, *Progr. Magn. Reson. Spetrosc.*, 1990, **22**, 453.
42 C. R. Cornman, G. J. Colpas, J. D. Hoeschele, J. Kampf and V. L. Pecoraro, *J. Am. Chem. Soc.*, 1992, **114**, 9925.
43 T. S. Smith II, R. L. LoBrutto and V. L. Pecoraro, *Coord. Chem. Rev.*, 2002, **228**, 1–18.
44 A. J. Tasiopoulos, A. N. Troganis, A. Evangelou, C. P. Raptopoulou, A. Terzis, Y. Deligiannakis and T. A. Kabanos, *Chem.–Eur. J.*, 1999, **5**, 910.
45 (*a*) I. Cavaco, J. Costa Pessoa, D. Costa, M. T. Duarte, R. D. Gillard and P. Matias, *J. Chem. Soc., Dalton Trans.*, 1994, 149; (*b*) G. Asgedom, A. Sreedhara, J. Kivikoski, J. Valkonen and C. P. Rao, *J. Chem. Soc., Dalton Trans.*, 1995, 2459.
46 W. Plass, A. Pohlmann and H.-K. Yozgatli, *J. Inorg. Biochem.*, 2000, **80**, 181.
47 M. R. Maurya, S. Agarwal, C. Bader, M. Ebel and D. Rehder, *Dalton Trans.*, 2005, 537.
48 M. R. Maurya, S. Khurana, C. Schulzke and D. Rehder, *Eur. J. Inorg. Chem.*, 2002, 779.
49 G. J. Colpas, B. J. Hamstra, J. W. Kampf and V. L. Pecoraro, *Inorg. Chem.*, 1994, **33**, 4669.
50 A. Giacomelli, C. Floriani, A. O. De Souza Duarte, A. Chiesi-Villa and C. Guastino, *Inorg. Chem.*, 1982, **21**, 3310.
51 M. Kosugi, S. Hikichi, M. Akita and Y. Moro-oka, *Inorg. Chem.*, 1999, **38**, 2567.
52 (*a*) A. Messerschmidt, L. Prade and R. Wever, *Biol. Chem.*, 1997, **378**, 309; (*b*) S. Macedo-Ribeiro, W. Hemrika, R. Renirie, R. Wever and A. Messerschmidt, *JBIC, J. Biol. Inorg. Chem.*, 1999, **4**, 209.
53 A. M. Ramadan, *J. Inorg. Biochem.*, 1997, **65**, 183 and references therein.
54 (*a*) V. Hulea and E. Dumitriu, *Appl. Catal., A*, 2004, **277**, 99; (*b*) Z. Fu, D. Yin, Q. Li, L. Zhang and Y. Zhang, *Microporous Mesoporous Mater.*, 1999, **29**, 351.
55 G. M. Sheldrick, *SHELXTL-NT V.5.1*, Bruker Analytical X-Ray Instruments Inc., Madison, WI, 1989.